Associative Behavior-Based abundance Index (ABBI) for yellowfin tuna (*Thunnus albacares*) in the Western Indian Ocean.

Yannick Baidai[1], Laurent Dagorn[1], Daniel Gaertner[1], Jean-Louis Denebourg[2], Antoine Duparc[1], Laurent Floch[1], and Manuela Capello[1]

ABSTRACT

This paper presents an associative behavior-based abundance index (ABBI) providing direct estimates of the abundance of yellowfin tuna (*Thunnus albacares*) based on their associative behavior around floating objects (FOBs). Considering the associative dynamics of small yellowfin tuna individuals (<10 kg) at FOBs through residence and absence times at FOBs, together with acoustic data obtained from fisher's echosounder buoys, the ABBI index is derived for yellowfin tuna in the western Indian Ocean over the period 2013-2019. This index accounts for both the FOB-associated and free-swimming components of the tuna populations, as well as for the effects of increasing numbers of FOBs on each component.

Keywords: *Abundance Index; Associative behavior; FADs; Yellowfin tuna*

1. INTRODUCTION

The availability to scientists of new data obtained from echosounder buoys has recently allowed the development of new methods for deriving alternative abundance indices of tropical tuna populations (Capello *et al.*, 2016; Santiago *et al.*, 2019). These methods offer complementary indices for the stock assessment of tropical tunas, with respect to the traditional Catch per Unit Effort (CPUE) indices. In the tropical tuna purse-seine fisheries, the rapid evolution of fishing efficiency and fleet dynamics resulting from the fast technological developments (Gaertner and Pallares, 1998; Torres-Irineo *et al.*, 2014), as well as the sharp increase in the use of drifting Fish Aggregating Devices (DFADs) since the 1990s, have significantly affected the fishing effort and complexified the derivation of CPUE abundance indices obtained from DFAD-

[1] MARBEC, Univ Montpellier, CNRS, Ifremer, IRD, Sète, France

[2] Unit of Social Ecology, Université Libre de Bruxelles (ULB), Bruxelles, Belgium

related catches. Defined as man-made floating objects, specifically designed to attract and concentrate tunas, DFADs are typically equipped with tracking technology (GPS) and echosounder buoys to remotely detect the associated tuna biomass and their location (Lopez *et al*., 2014). DFADs have considerably increased the catchability of tropical tuna species and are considered as one of the most important changes that have contributed to the increase in the efficiency of purse seiners (Fonteneau *et al*., 2013). However, the non-random nature of this fishing method has resulted in considerable complexity in estimating fishing effort in the purse seine fishery. This situation highlights the need for novel, effort-independent data and indicators, notably directed towards the development of alternative methods to improve the abundance assessment of tropical tuna populations.

Recent studies based on the new data provided by echosounder buoys, allowed assessing the accuracy of the biomass estimates provided by several buoy brands and models (Lopez *et al.*, 2016; Baidai *et al.*, 2017, 2020a; Diallo *et al.*, 2019; Orue *et al.*, 2019). These studies demonstrated that accurate estimates on the presence/absence of tuna at the FADs can be obtained. Models of tuna behavior within FAD arrays were developed (Capello *et al.*, 2016), allowing to express the ratio between the FAD-associated and total tuna population in terms of the amount of time spent by tuna individuals associated at FADs (residence times) and unassociated (absence times). Furthermore, acoustic tagging experiments conducted on DFADs allowed assessing the residence times for tropical tuna species in the Indian ocean (Govinden *et al.*, 2021).

Building on these recent findings, we propose a new population assessment method for yellowfin tuna based on their associative behavior with floating objects: the Associative Behavior-Based abundance Index (ABBI). The ABBI relies on the modelling framework introduced by Capello *et al.* (2016), that combines the occupancy of floating objects by tuna aggregations, measured from acoustic data collected by fishers' buoys on DFADs, with the associative metrics of tuna individuals obtained from acoustic tagging data, in order to provide direct estimates of the abundance of tropical tuna populations. In the following, the ABBI index was derived over the period 2013-2019, for the small yellowfin tuna (*Thunnus albacares*) (< 10 Kg) in the Western Indian Ocean (WIO).

2. MATERIALS AND METHODS

2.1. Model definition

The associative behaviour of tropical tuna implies that tuna schools can be in two states, either associated with FADs, or not associated, i.e., in the so-called free-swimming state. At any given time t, the overall abundance of tuna (N) in a given area, results from the sum of the abundances of two components: the associated (X_a) and the free-swimming populations (X_u).

$$N(t) = X_a(t) + X_u(t) \tag{1}$$

Within a given study region and time period, the average associated tuna population ($\overline{X_a}$) can be estimated as follows:

$$\overline{X_a} = \bar{m}\bar{f}\bar{p} \tag{2}$$

where m is the average tuna biomass found under the inhabited FOBs in the study region (*i.e.*, a FOB occupied by tuna), f represents the proportion of inhabited FOBs by the tuna species and p the total number of FOBs in the region of interest. In the above equation, the symbol "$\bar{}$" denotes the time average. Capello *et al.*, (2016) demonstrated that, by measuring the continuous bout of times that tunas spend unassociated or associated to a FOB, i.e., respectively, the continuous absence time and the continuous residence time, it is possible to estimate the ratio between the average associated and total tuna population within a given area:

$$\frac{\overline{X_a}}{\overline{N}} = \frac{CRT}{CRT + CAT} \tag{3}$$

where *CRT* denotes the average continuous residence times, i.e. continuous bouts of time that tuna spend associated to FOBs and *CAT* denotes the average continuous absence times, *i.e.* continuous bout of times that tuna spend in the free-swimming state. Because the amount of time that tuna spends associated at FADs (or out of them) can be species and size-dependent, Equation (3) is valid for tuna species and size classes that manifest the same associative behavior with FOBs. In the following, we will consider small (< 10 kg) yellowfin tuna (*Thunnus albacares*), whose associative behaviour with FOBs has been studied within acoustic tagging experiments within arrays of drifting and anchored FADs (Table 1).

Considering Eqs. (2-3), the total tuna population within an area can be estimated as:

$$\overline{N} = \frac{CRT + CAT}{CRT}\bar{m}\bar{f}\bar{p} \tag{4}$$

Furthermore, considering Eqs. (1-2) and (4), the free-swimming population (X_u) can be expressed from the following relation:

$$\overline{X_u} = \frac{CAT}{CRT}\bar{m}\bar{f}\bar{p} \quad (5)$$

2.2. Study area and period

The study area extended between latitudes 10° S and 10° N and covered longitudes located between the African coasts and 70° E (Figure 1). The study considers years 2013-2019, where echosounder buoys data are available. The analysis was conducted on a quarterly basis, considering a spatial grid of 10°.

2.3. Field data

2.3.1. FOB-associated average tuna biomass (m)

The average biomass of small yellowfin tuna (i.e. less than 10 kg or YFT-10kg), around an inhabited FOB (i.e., a FOB occupied by a tuna aggregation), in the study area was estimated from DFAD catch and sampling data (Table 1). The catch data were corrected using the T3 processing (Pallarés and Petit, 1998; Duparc *et al.*, 2018). The catch corrections firstly involve raising the catches from the logbook, using the weights reported in the landing notes. Secondly, the species composition derived from well samples, was extrapolated at the fishing set level according to the proportionality of the catch set in the well (see details in Duparc *et al.*, 2018). During this step, the length-weight, relationships, with official IOTC parameters (IOTC, 2020) were used for each species. The catch by species was then computed for each sampled set.

Since the catches for all yellowfin tuna size classes are aggregated in the T3 process, the proportion of YFT-10kg were calculated based on the size distribution in samples. The average set biomass of small yellowfin tuna was then derived from the product of the average DFAD catch of this species, by the average biomass proportion of individuals under 10 kg in the samples. Averages of catches and proportions of YFT-10kg were only calculated considering a minimum threshold of 10 available data per time/area unit. This method was applied for each spatio-temporal strata (i.e. 10° square and quarter, see details in 2.4 section). All data were provided by Ob7 – "Observatoire des Ecosystèmes Pélagiques Tropicaux exploités". The data were collected through the Data Collection Framework (Reg 2017/1004 and 2016/1251) funded by both IRD and the European Union.

2.3.2. Proportion of inhabited FOBs (f)

Acoustic data collected by the Marine Instruments M3I buoys were translated into presence/absence of a tuna aggregation, using a machine learning algorithm (Baidai *et al.*, 2020), that was shown to provide good accuracies (85%) in the Indian Ocean. The first sections of presence or absence occurring at the beginning of the FAD trajectories were excluded from the analysis as they may result from the colonization period of the DFAD during which the DFAD-tuna system is not yet at equilibrium, or potentially from classification errors related to the operation on the buoy (Baidai *et al.*, 2020a).

Daily presence/absence data were then used to derive the proportion of FOBs inhabited by a tuna aggregation (f). This was expressed as the number of DFADs (equipped by an M3I buoy) classified as inhabited by a tuna aggregation, divided by the total number of M3I buoys at a daily scale. A threshold of at least 10 available buoys per day and space-time unit was considered for the calculation of the daily proportion of inhabited FOBs. Table 2 provides the average daily numbers of available M3I buoys used over the study area. Quarterly averages of the proportion of inhabited FOBs were then calculated. Because an accurate species discrimination from these acoustic data was not possible, these values were corrected with the occurrence of YFT-10 kg in the FOB-associated tuna aggregations, according to Eq. (6):

$$f(\text{YFT-10 kg}) = f.\eta(\text{YFT-10 kg}) \quad (6)$$

where $\eta(\text{YFT-10 kg})$ represents the ratio between the number of DFAD-catches containing a biomass greater than or equal to 1 ton of YFT-10 kg, relative to the total number of positive DFAD sets. This ratio was estimated on a quarterly basis, within each grid cell, using the sampling data raised to the catch per set. A minimum number of 10 available sampling data per strata was considered for the ratio calculation.

2.3.3. Continuous residence time of yellowfin tuna (CRT)

Continuous residence times (CRT) of yellowfin tuna have been well documented in the three oceans, on both anchored and drifting FADs (see Table 3). In the Indian Ocean, acoustic tagging experiments were carried out around drifting FADs by Govinden *et al.*, (2021), on yellowfin tuna individuals in the Mozambique Channel (mean fork length ±SD: 65±22 cm, n=16) and in the Seychelles area (mean fork length ±SD: 59±9 cm, n = 15). This study revealed that yellowfin tunas remain associated 6.64 days on average around the same DFADs. This average value was considered in this study.

2.3.4. Continuous absence time of yellowfin tuna (CAT)

Currently, CRTs around DFADs could be estimated through acoustic tagging for the three main tuna species (Dagorn *et al.*, 2007; Matsumoto *et al.*, 2014, 2016; Scutt *et al.*, 2019; Tolotti *et al.*, 2020; Govinden *et al.*, 2021). However, no direct measurement of yellowfin CATs has yet been carried out on DFADs in the study area. Only experiments conducted on anchored FAD arrays could estimate CATs so far. However, recent studies demonstrated decreasing CATs for increasing numbers of FOBs (Rodriguez-Tress *et al.*, 2017; Pérez *et al.*, 2020). An intuitive argument that explains how the time spent by tuna between two FOB associations (the CAT) depends on the FOB densities, relies on the fact that the FOB encounter rates by a tuna are smaller (i.e., larger CATs) when the distances between FOBs are larger (i.e., smaller FOB densities). From these findings, the CAT was related to the number of FOBs according to the following ansatz:

$$CAT = \frac{1}{\phi p} \tag{7}$$

Where $\boldsymbol{\phi}$ is a parameter that relates the number of FOBs (p) to the CAT. The CAT values were then derived from (Eq. 7), considering the estimated number of FOBs (see next section) and different ϕ values ranging between 2e-5 and 5e-4. A detailed section on the significance and plausible magnitude order of ϕ is provided in Appendix (The ϕ significance).

2.3.5. Total number of floating objects (p)

Estimating the total number of floating objects (p) constituted one of the main challenges of this approach. Although the GPS satellite communication technology integrated in the echosounder buoys equipping DFADs can allow reconstructing densities of instrumented floating objects at fine spatial and temporal scales, the commercial and strategic nature of these data for purse seiners represents a major limitation to their full availability to scientists. Consequently, the number of FOBs in each of the time-area units was assessed from the number of buoys equipping the DFADs deployed by the French tuna purse seine fleet, and two raising factors. First, the estimates of the total number of DFADs were calculated from the ratios between DFADs deployed by French and Spanish purse-seiners fleets, provided from 2010 to the end of 2017, by Katara *et al.* (2018). The missing ratios for the years 2018 and 2019 were estimated using the average ratio over the year 2017, based on the assumption of a relative stabilization in the exploitation of buoys between the different fleets after this period (limitation

measures on the number of buoys operated by tuna purse-seiners in the Indian Ocean: IOTC Resolutions 15/08 and 17/08). The total number of FOBs in each time-area unit was then derived from the ratios of DFADs encountered by observers on-board French tuna seiners, relative to other natural (marine mammals, trees, etc.) or artificial (debris from human activities) floating objects. Observer data were collected under the EU Data Collection Framework (DCF) and the French OCUP program (Observateur Commun Unique et Permanent), with an overall average coverage rate of about 50% over the years 2013 to 2017 (Goujon *et al.*, 2017).

2.4. Abundance estimates

Abundance estimates were conducted considering a spatio-temporal stratification of 10° quarter. In each 10 ×10° grid cell, the associated, free-swimming and total YFT-10kg abundance was calculated following respectively the Eqs. (2), (5) and (4). For each component (associated, free-swimming and total), an average quarterly index was then estimated for the full study area, considering the average over the spatial strata with available data for the same period. Relative abundance indices for the different components are also provided, considering the first quarter of the year 2013 as reference and different values of ϕ (for the total population).

3. RESULTS AND DISCUSSION

3.1. Time series of abundance of juvenile yellowfin tuna in the WIO

Figures 2 and 3 show, respectively, the absolute and relative abundance estimates of the total population of YFT -10kg per 10° square, and its associated and free-swimming components. They reveal that globally both components of the YFT-10kg population (associated and free-swimming tunas) appear to follow roughly similar trajectories characterized by remarkable biomass drops during the years 2014-2015, and 2019. The variation of the ϕ values used for the free-swimming and the total population, did not change the trends of the estimated biomass qualitatively. However, the variability of the relative ABBI index was lower for small ϕ values (i.e. less than or equal to 5e-5), which are the most plausible (Appendix A1). Details on the ABBI index inputs for each stratum can be found in Appendix A2.

From a set of descriptive metrics of the associative behaviour of tunas around floating objects (namely residence and absence times) and the occupancy rate of these objects by tuna aggregations, this novel approach thus provided direct, effort-independent and absolute

abundance indices for small yellowfin tuna (-10Kg) in the Western Indian Ocean. However, data collection represented one of its major challenges. Current collection of tuna continuous residence times (CRT) is usually related to short-term projects, and remains limited to specific oceanic regions and periods. Similarly, although the technology exists to allow for the measurement of tuna continuous absence time (*CAT*), this metric has so far received very little attention and there is currently a critical need of knowledge on this essential data to understand the associative behaviour of tuna (Dagorn *et al.*, 2007; Robert *et al.*, 2012, 2013; Rodriguez-Tress *et al.*, 2017). Additional efforts for regular and large-scale electronic tagging programs would be critical to provide a better understanding of the associative behavior of tunas, and to carry out accurate assessments of their populations based on the ABBI methodology.

The availability of data on FOBs represented also a major limitation encountered in this study. DFADs actually constitute the main component of the total floating objects in the Indian Ocean, as indicated by the work from Dagorn *et al.*, (2013b), and corroborated by the results from this study (see Appendix: Figure A2.4 and A2.5). Currently all DFADs are equipped with satellite linked echosounder buoys (Lopez *et al.*, 2014; Moreno *et al.*, 2019), whose geolocation data could allow to reconstruct densities of floating objects at fine spatial and temporal scales. However, availability of these data still remain problematic, and relatively limited depending on the fleets, companies or buoy manufacturers (Moniz and Herrera, 2019; Grande *et al.*, 2020). As a result, the total number of DFADs at water remains poorly documented and globally unknown.

Nevertheless, these different issues do not detract from the potential of this new alternative for tropical tuna population assessment. To date, the data required for this approach are mainly devoted to either improve general knowledge on the ecology of tuna species (behavioural metrics) or for regulatory purposes (number of DFADs). The possibility of deriving from these data, abundance indices independent of the fishing effort could support future developments of dedicated data collection programs.

ACKNOWLEDGEMENTS

This project as co-funded by the ANR project BLUEMED (ANR-14-ACHN-0002) and "Observatoire des Ecosystèmes Pélagiques Tropicaux exploités" (Ob7) from IRD/MARBEC. The authors are grateful to ORTHONGEL and its contracting parties (CFTO, SAPMER,

SAUPIQUET) for providing the echosounder buoys data. The authors also thank all the skippers who gave time to share their experience and knowledge on the echosounder buoys. The authors sincerely thank the contribution of the staff of the Ob7 on the databases of the echosounder buoys. We are also deeply grateful to the buoy manufacturers for their useful advice and information on their echosounder buoys.

REFERENCES

Baidai, Y., Capello, M., Billet, N., Floch, L., Simier, M., Sabarros, P., and Dagorn, L. 2017. Towards the derivation of fisheries-independent abundance indices for tropical tunas: Progress in the echosounders buoys data analysis. IOTC-2017-WPTT19-22 Rev1, IOTC-2017-WPTT19-22 Rev1. Mahé. 12 pp. http://www.iotc.org/documents/towards-derivation-abundance-indices-tropical-tuna-recent-progress-analysis-echosounder.

Baidai, Y., Dagorn, L., Amande, M. J., Gaertner, D., and Capello, M. 2020a. Aggregation processes of tuna under Drifting Fish Aggregating Devices (DFADs) assessed through fisher's echosounder buoy in the Atlantic Ocean. Collected Volume of Scientific Papers ICCAT, 76: 762–776.

Baidai, Y., Dagorn, L., Amande, M. J., Gaertner, D., and Capello, M. 2020b. Machine learning for characterizing tropical tuna aggregations under Drifting Fish Aggregating Devices (DFADs) from commercial echosounder buoys data. Fisheries Research, 229: 105613. Elsevier. https://doi.org/10.1016/j.fishres.2020.105613.

Capello, M., Deneubourg, J. L., Robert, M., Holland, K. N., Schaefer, K. M., and Dagorn, L. 2016. Population assessment of tropical tuna based on their associative behavior around floating objects. Scientific Reports, 6: 1–14. The Author(s). http://dx.doi.org/10.1038/srep36415.

Dagorn, L., Pincock, D., Girard, C., Holland, K., Taquet, M., Sancho, G., Itano, D., et al. 2007. Satellite-linked acoustic receivers to observe behavior of fish in remote areas. Aquatic Living Resources, 20: 307–312. http://www.alr-journal.org/10.1051/alr:2008001.

Dagorn, L., Bez, N., Fauvel, T., and Walker, E. 2013. How much do fish aggregating devices (FADs) modify the floating object environment in the ocean? Fisheries Oceanography, 22: 147–153.

Diallo, A., Baidai, Y., Manocci, L., and Capello, M. 2019. Towards the derivation of fisheries-independent abundance indices for tropical tuna: Report on biomass estimates obtained from a multi-frequency echosounder buoy model (M3I+). IOTC-2019-WPTT21-54_Rev1. 36 pp.

Duparc, A., Cauquil, P., Depetris, M., Dewals, P., Floch, L., Gaertner, D., Hervé, A., et al. 2018. Assessment of accuracy in processing purse seine tropical tuna catches with the T3 methodology using French fleet data: 1–19.

Fonteneau, A., Chassot, E., and Bodin, N. 2013. Global spatio-temporal patterns in tropical tuna purse seine fisheries on drifting fish aggregating devices (DFADs): Taking a historical perspective to inform current challenges. Aquatic Living Resources, 26: 37–48. EDP Sciences. https://www.cambridge.org/core/article/global-spatiotemporal-patterns-in-tropical-tuna-purse-seine-fisheries-on-drifting-fish-aggregating-devices-dfads-taking-a-historical-perspective-to-inform-current-challenges/0A00E8E2AA3D636D1F5F48577AB6DF7A.

Gaertner, D., and Pallares, P. 1998. Efficiency of Tuna Purse-Seiners and Effective Effort/Efficacité des thoniers senneurs et efforts réels"(ESTHER).

Goujon, M., Maufroy, A., Relot-Stirnemann, A., Moëc, E., Bach, P., Cauquil, P., Sabarros, P., et al. 2017. Collecting data on board French and Italian tropical tuna purse seiners with common observers: results of ORTHONGEL'S voluntary observer program OCUP (2013-

2017) in the Indian ocean. IOTC-2017-WPDCS13-22_Rev1. 22 pp. https://www.iotc.org/sites/default/files/documents/2017/11/IOTC-2017-WPDCS13-22_Rev1_-_OBS_PS_FRA.pdf.

Govinden, R., Capello, M., Forget, F., Filmalter, J. D., and Dagorn, L. 2021. Behavior of skipjack (Katsuwonus pelamis), yellowfin (Thunnus albacares), and bigeye (T. obsesus) tunas associated with drifting fish aggregating devices (dFADs) in the Indian Ocean, assessed through acoustic telemetry. Fisheries Oceanography: fog.12536. https://onlinelibrary.wiley.com/doi/10.1111/fog.12536.

Grande, M., Capello, M., Baidai, Y., Uranga, J., Boyra, G., Quincoces, I., Orue, B., et al. 2020. From fishermen to scientific tools: progress on the recovery and standardized processing of instrumented buoys data. Collected Volume of Scientific Papers ICCAT, 76: 881–891.

IOTC-WPTT22(DP). 2019. Report of the 22nd Session of the IOTC Working Party on Tropical Tunas. Online, 22-24 June 2020. IOTC–2020–WPTT22(DP)–R[E]. 35 pp.

IOTC, 2020. Estimation of catches at size for IOTC species. IOTC-2020-WPTT22-DATA13. Available at: https://www.iotc.org/WPTT/22DP/Data/13-Equations;

Katara, I., Gaertner, D., Marsac, F., Grande, M., Kaplan, D., Agurtzane, U., Loreleï, G., et al. 2018. Standardisation of yellowfin tuna CPUE for the EU purse seine fleet operating in the Indian Ocean. IOTC–2018–WPTT20–36_Rev1. 1–14 pp.

Lopez, J., Moreno, G., Sancristobal, I., and Murua, J. 2014. Evolution and current state of the technology of echo-sounder buoys used by Spanish tropical tuna purse seiners in the Atlantic, Indian and Pacific Oceans. Fisheries Research, 155: 127–137. http://dx.doi.org/10.1016/j.fishres.2014.02.033.

Lopez, J., Moreno, G., Boyra, G., and Dagorn, L. 2016. A model based on data from echosounder buoys to estimate biomass of fish species associated with fish aggregating devices. Fishery Bulletin, 114: 166–178. https://spo.nmfs.noaa.gov/content/model-based-data-echosounder-buoys-estimate-biomass-fish-species-associated-fish-aggregating.

Matsumoto, T., Satoh, K., and Toyonaga, M. 2014. Behavior of skipjack tuna (Katsuwonus pelamis) associated with a drifting FAD monitored with ultrasonic transmitters in the equatorial central Pacific Ocean. Fisheries Research, 157: 78–85. Elsevier B.V. http://dx.doi.org/10.1016/j.fishres.2014.03.023.

Matsumoto, T., Satoh, K., Semba, Y., and Toyonaga, M. 2016. Comparison of the behavior of skipjack (Katsuwonus pelamis), yellowfin (Thunnus albacares) and bigeye (T. obesus) tuna associated with drifting FADs in the equatorial central Pacific Ocean. Fisheries Oceanography, 25: 565–581. http://doi.wiley.com/10.1111/fog.12173.

Moniz, I., and Herrera, M. 2019. Using FADs to develop better abundance indices for tropical tuna. Collect. Vol. Sci. Pap. ICCAT, 75: 2196–2201.

Moreno, G., Boyra, G., Sancristobal, I., Itano, D., and Restrepo, V. 2019. Towards acoustic discrimination of tropical tuna associated with Fish Aggregating Devices. PLOS ONE, 14: e0216353. http://dx.plos.org/10.1371/journal.pone.0216353.

Orue, B., Lopez, J., Moreno, G., Santiago, J., Boyra, G., Soto, M., and Murua, H. 2019. Using fishers' echo-sounder buoys to estimate biomass of fish species associated with drifting fish aggregating devices in the Indian Ocean. Revista de Investigación Marina, AZTI, 26: 1–13.

Pallarés, P., and Petit, C. 1998. Tropical tunas: new sampling and data processing strategy for estimating the composition of catches by species and sizes. Collect. Vol. Sci. Pap. ICCAT, 48: 230–246.

Pérez, G., Dagorn, L., Deneubourg, J. L., Forget, F., Filmalter, J. D., Holland, K., Itano, D., et al. 2020. Effects of habitat modifications on the movement behavior of animals: the case study of Fish Aggregating Devices (FADs) and tropical tunas. Movement Ecology, 8: 1–11. Movement Ecology.

Robert, M., Dagorn, L., Deneubourg, J. L., Itano, D., and Holland, K. 2012. Size-dependent behavior of tuna in an array of fish aggregating devices (FADs). Marine Biology, 159: 907–914.

Robert, M., Dagorn, L., Lopez, J., Moreno, G., and Deneubourg, J. L. 2013. Does social behavior influence the dynamics of aggregations formed by tropical tunas around floating objects? An experimental approach. Journal of Experimental Marine Biology and Ecology, 440: 238–243.

Rodriguez-Tress, P., Capello, M., Forget, F., Soria, M., Beeharry, S., Dussooa, N., and Dagorn, L. 2017. Associative behavior of yellowfin Thunnus albacares, skipjack Katsuwonus pelamis, and bigeye tuna T. obesus at anchored fish aggregating devices (FADs) off the coast of Mauritius. Marine Ecology Progress Series, 570: 213–222. http://www.int-res.com/abstracts/meps/v570/p213-222/.

Santiago, J., Uranga, J., Quincoces, I., Orue, B., Merino, G., Murua, H., and Boyra, G. 2019. A novel index of abundance of juvenile yellowfin tuna in the Atlantic Ocean derived from echosounder buoys. 2nd Joint t-RFMO FAD Working Group meeting: 24.

Scutt, P., Leroy, B., Peatman, T., Escalle, L., and Smith, N. 2019. Electronic tagging for the mitigation of bigeye and yellowfin tuna juveniles by purse seine fisheries. WCPFC-SC15-2019/EB-WP-08. 19 pp.

Tolotti, M. T., Forget, F., Capello, M., Filmalter, J. D., Hutchinson, M., Itano, D., Holland, K., et al. 2020. Association dynamics of tuna and purse seine bycatch species with drifting fish aggregating devices (FADs) in the tropical eastern Atlantic Ocean. Fisheries Research, 226: 105521. https://doi.org/10.1016/j.fishres.2020.105521.

Torres-Irineo, E., Gaertner, D., Chassot, E., and Dreyfus-León, M. 2014. Changes in fishing power and fishing strategies driven by new technologies: The case of tropical tuna purse seiners in the eastern Atlantic Ocean. Fisheries Research, 155: 10–19. http://dx.doi.org/10.1016/j.fishres.2014.02.017.

Tables

Table 1: Number of FOB sets per quarter used to estimate the average biomass of yellowfin tuna at FOBs in the study area. The third column indicated the total number of FOB fishing sets from the logbook data corrected with the T3 process. The last column indicates the number of sampled fishing sets used to (i) estimate the proportion of yellowfin tuna (<10Kg) catches in each stratum and (ii) correct the proportion of occupied buoys (f) using equation (6).

Year	Quarter	FOB sets	Sampled FOB sets
2013	Q1	167	54
	Q2	236	90
	Q3	395	118
	Q4	548	159
2014	Q1	344	95
	Q2	240	57
	Q3	537	154
	Q4	451	106
2015	Q1	154	12
	Q2	194	12
	Q3	466	87
	Q4	621	101
2016	Q1	352	68
	Q2	296	35
	Q3	613	127
	Q4	610	60
2017	Q1	403	16
	Q2	478	73
	Q3	675	120
	Q4	633	154
2018	Q1	679	173
	Q2	541	170
	Q3	662	262
	Q4	668	0
2019	Q1	491	131
	Q2	257	39
	Q3	542	70
	Q4	738	168

Table 2: Daily average number of French M3I buoys and total number of French buoys in the study area by quarter used to estimate the proportion of FOB inhabited by yellowfin tuna (<10Kg) and the total buoy number.

Year	Quarter	M3I Buoy Count	Total buoy count
2013	Q1	331	426
	Q2	349	491
	Q3	493	690
	Q4	377	674
2014	Q1	328	747
	Q2	450	939
	Q3	517	987
	Q4	667	1134
2015	Q1	633	944
	Q2	999	1352
	Q3	1328	1621
	Q4	1492	1735
2016	Q1	1720	1945
	Q2	1712	1878
	Q3	1709	1836
	Q4	2100	2194
2017	Q1	2074	2227
	Q2	1723	2332
	Q3	2028	2849
	Q4	1937	2544
2018	Q1	1916	2372
	Q2	2014	2508
	Q3	2073	2701
	Q4	2190	2875
2019	Q1	1984	2813
	Q2	1787	2496
	Q3	1790	2516
	Q4	1736	2609

Table 3: Summary of main findings from previous studies on yellowfin tuna individual CRT assessed under an anchored and under an drifting FADs (FL: Fork length).

Study	Location	Species	FL range (cm)	CRT
Dagorn *et al.*, (2007)	Western Indian Ocean	YFT	*Not provided*	Average at 1.04 days (maximum: 15.22 days)
Govinden *et al.*, (2021)	Western Indian Ocean	YFT	29 – 111	Median at 6.64 days (maximum: 26.72 days)
Matsumoto *et al.*, (2016)	Equatorial central Pacific Ocean	YFT	31.6 – 93.5	Average at 4.1 days (maximum 14.5 days)
Scutt *et al.*, (2019)	Western Central Pacific Ocean	YFT	36 – 98	Median at 2 days (maximum: 50 days)
Tolotti *et al.*, (2020)	Eastern Atlantic Ocean	YFT	34 – 82	Average at 19.15 days (maximum value to 55 days)

Figures

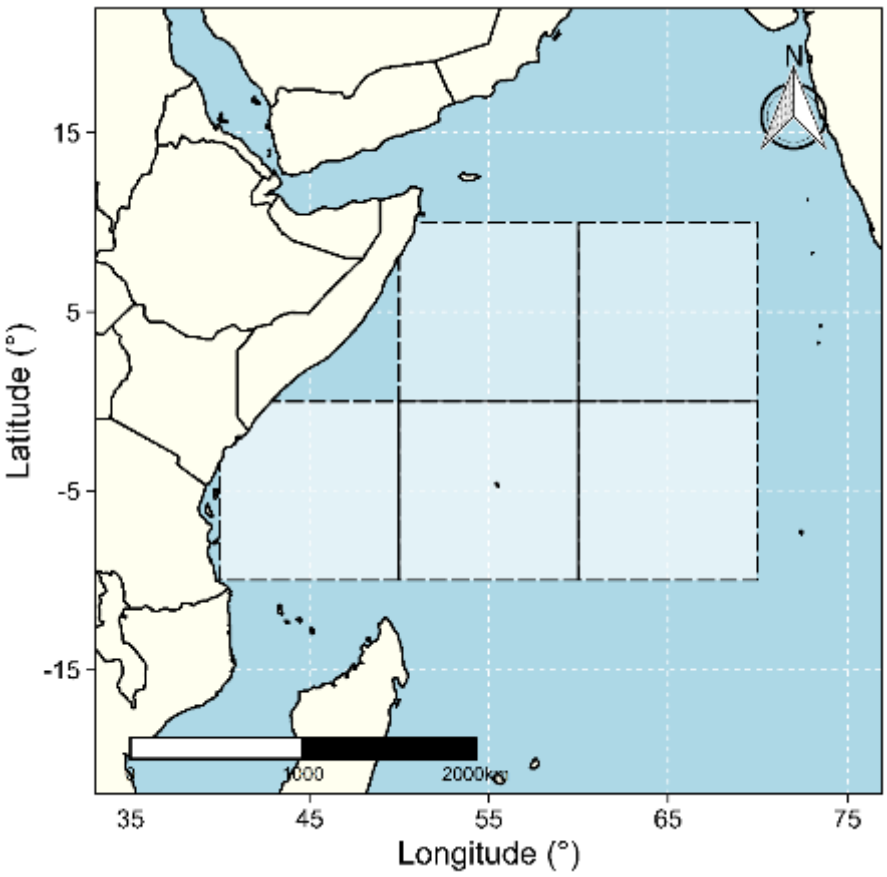

Figure 1: Spatial stratification of the study area

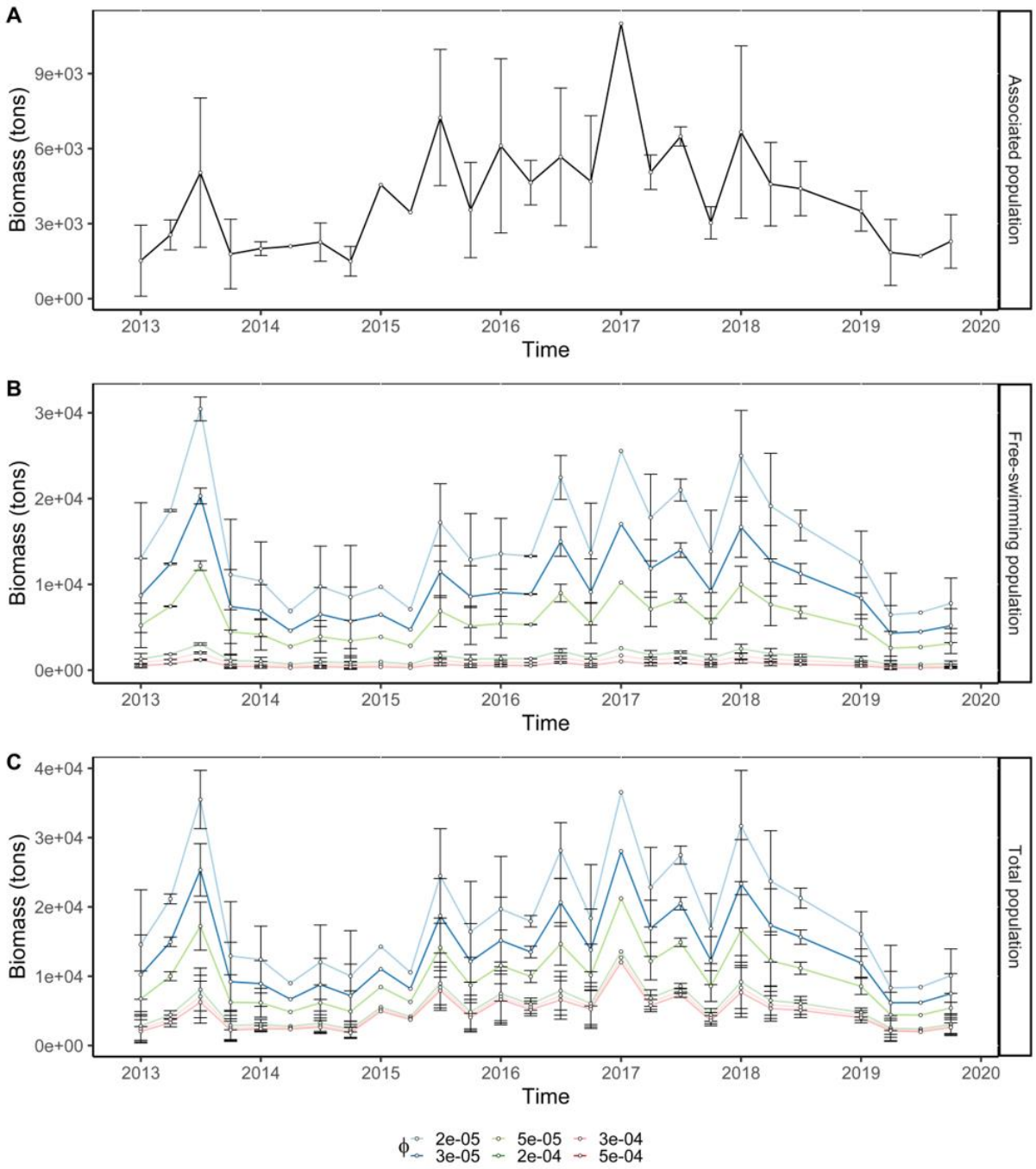

Figure 2: Time series of the average absolute abundances per 10° square of the YFT-10kg over 2013-2019. (A) Absolute abundances of the associated component, (B) Absolute abundances of the free-swimming component and (C) and the total population ABBI under different values of ϕ.

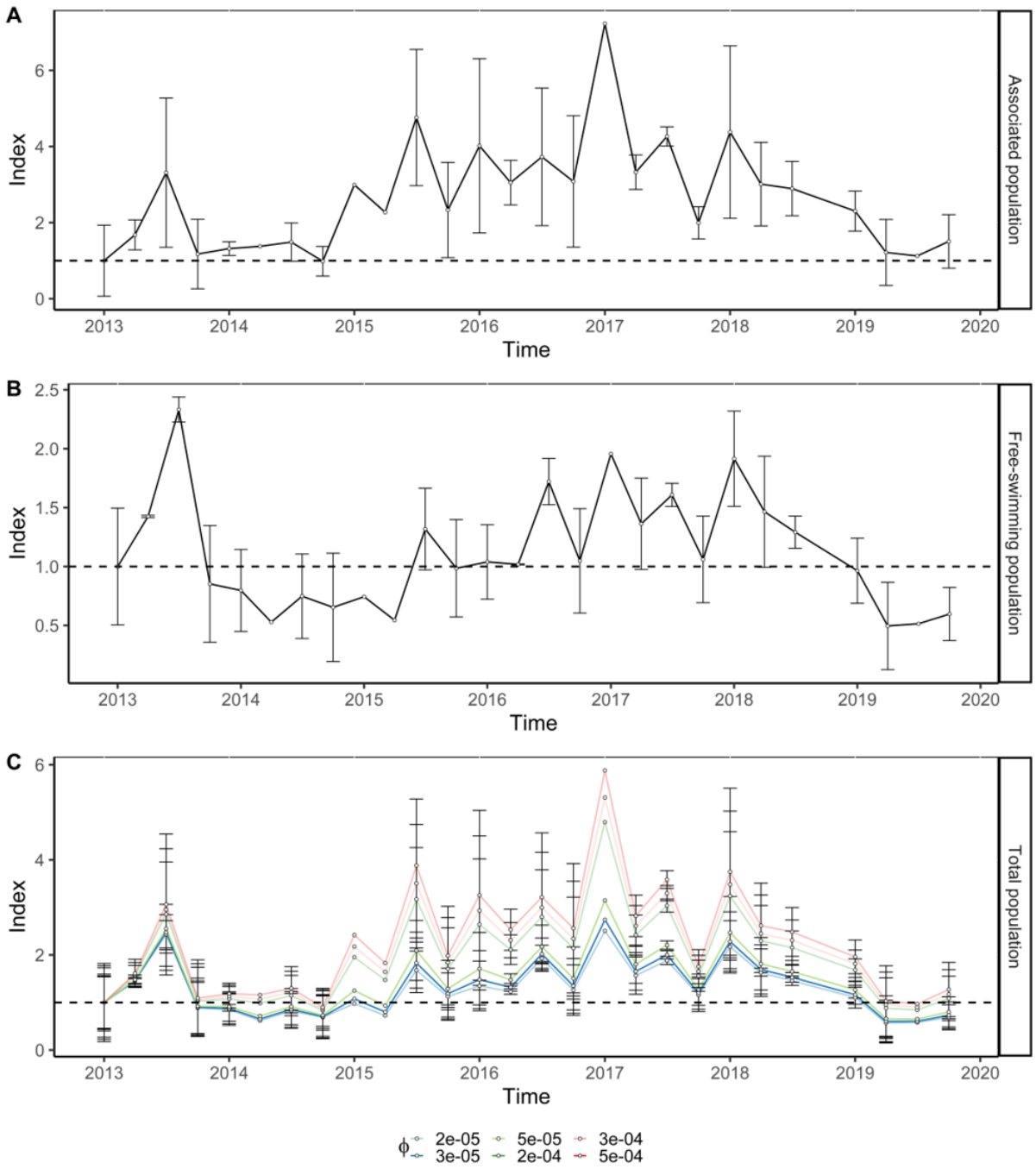

Figure 3: Time series of the relative abundances per 10° square of the YFT-10kg over 2013-2019. (A) Relative abundance of the associated component. (B) Relative abundances of the free-swimming component (E) and the total population under different values of ϕ. Relative abundances were estimated considering the first quarter of 2013 as reference value.

Appendix A1: The ϕ significance

Currently, there are no reliable observational data for CAT of tropical tunas, one of the main variables used in the proposed abundance assessment model. To overcome this limitation, the relation between CAT and the number of FOBs in the system has been estimated based on an *ansatz* introducing the parameter ϕ. This parameter is intended to move from the local scale at which associative processes take place (where the CAT are measured), to the scale of oceanic regions considered for the abundance estimates (where the number of FOBs is estimated). Indeed, following Capello *et al.*, (2016), for a system at equilibrium, the CAT can be related to the number of FOBs in the system (p) and the association probability (μ_i), defined as the probability for a non-associated fish to associate with a FOB i, as follows

$$CAT = \frac{1}{\sum_{i=1}^{p} \mu_i} \qquad (A1)$$

However, at oceanic scales considered, the associative processes of a tuna can realistically only concern a limited number of FOBs (p_0), corresponding to those that the tuna may encounter locally following its departure from another FOB. Therefore, p_0 represents the number of FOBs likely to be locally visited by the tuna, and located in the area S_0 that can be explored by the tuna between two consecutive associations. Herein referred to as the "local interaction zone", S_0 thus corresponds to the basic space-time unit within which the associative processes of a tuna take place (Figure A1). It is assumed that within it, all FOBs have the same probability of being visited and hosting tuna. The CAT definition can therefore be rewritten according to the following equation:

$$CAT = \frac{1}{p_0 \mu_i} \qquad (A2)$$

Considering a homogeneous distribution of FOBs, it is possible to write:

$$\frac{p}{S} = \frac{p_0}{S_0} \qquad (A3)$$

where S represents the area of the oceanic scale considered for the abundance assessment. Inserting the above relation into the CAT definition provided at Equation (A2) leads to:

$$CAT = \frac{1}{\left(\frac{S_0}{S}\mu_i\right)p} \qquad (A4)$$

By considering CAT definition from Equation (7), it is therefore possible to express the parameter ϕ as the product of the surface ratio and the association probability:

$$\phi = \frac{S_0}{S}\mu_i \qquad (A5)$$

The area S_0 depends on the search dynamics of the tuna (random walk) and is currently unknown. However, it can be assumed that S_0 could be limited to the theoretical area that a tuna could cover during the basic unit of time considered (namely one day the time unit considered in this study). This would correspond to a circle with radius equal to the maximum distance travelled by a tuna in 24 hours (case of a "straight swim" to the FOB). Considering tunas moving at a constant speed of 1 BL/s (body length/s), for tunas of 50 cm, the local interaction area would thus extend to about 6,000 km². Considering the approximately 1,2 million km² of the 10°×10° squares considered as spatial units, the surface ratio S_0/S would therefore correspond approximately to 5e-3. Since μ_i in Equation (A5) is always < 1 (probability per unit time), the order of magnitude of S_0/S is consistent with the low values of ϕ (ϕ ~ 1e-5), and these values are therefore the most plausible for estimating the tuna abundances.

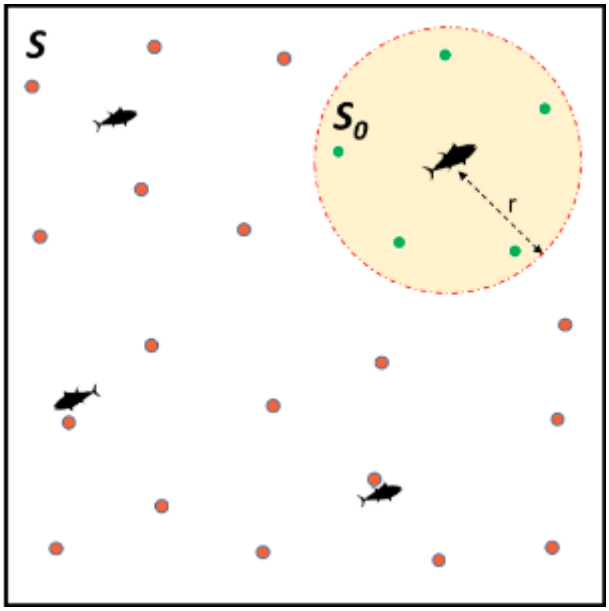

Figure A1.1: Schematic view of the local tuna environment. The green dots represent the FOBs with similar probabilities to be reached by the tuna located at the center of the circle. Conversely, the orange dots are the least likely to be reached by the same tuna. *S* and S_0 denotes respectively for the global zone and the local interaction zone of the tuna, and *r* represent the radius of the local interaction zone.

Appendix A2: Time series of model inputs

1. Time series of FOB-associated biomass (m) and proportion of inhabited FOBs (*f*(YFT-10kg))

The average biomass of YFT-10kg around an inhabited FOB appear relatively stable in the different time and area units, with average values varying between 6 and 8 tons (Figure A2.1). The coefficient $\eta(\text{YFT-10 kg})$, representing the ratio between the number of DFAD-catches containing a biomass greater than or equal to 1 ton of YFT-10 kg, relative to the total number of positive DFAD sets, is shown in Figure A2.2. Overall, amounts of YFT-10kg larger than 1 ton were present in an average of 84% of the tuna aggregations sampled in the whole area considered, with average values varying between 78 and 90%, in the different time-area units (Figure A2.2). The corrected proportions of floating objects hosting YFT-10kg, resulting from the estimated coefficient $\eta(\text{YFT-10 kg})$ and the proportions of FOBs inhabited by tuna aggregations (f) (see Eq.(6)), are presented in Figure A2.3.

2. Time series of the estimated number of FOBs (*p*)

The temporal evolution of the estimated number of FOBs revealed that DFADs constitute the main driver of FOB density in the study area, given the relative stability of percentage of "other" floating objects (including natural and artificial logs) over time (Figure A2.4).

Globally, the different time-area units were characterized by two main trends: (i) the period before 2015 characterized by a steady increase in the number of FOBs, and (ii) the period after 2015 with a plateau at about 2,000 FOBs on average, per 10x10° square (Figure A2.5).

3. Time series of continuous absence time (*CAT*)

The estimated continuous absence times (Eq.7) were relatively homogeneous over the different -time-area units considered. For ϕ values higher than or equal to 2e-4, YFT-10kg would have spent between 1 and 4 days on average in the free-swimming state, while ϕ values lower than 2e-4, provided CATs ranging between 14 and 33 days on average (Figure A2.6).

4. Abundance estimates per 10° square

The estimated abundances of the associated, free-swimming and the total YFT-10kg population over the different time area units are shown on Figures A2.7, A2.8, A2.9, respectively.

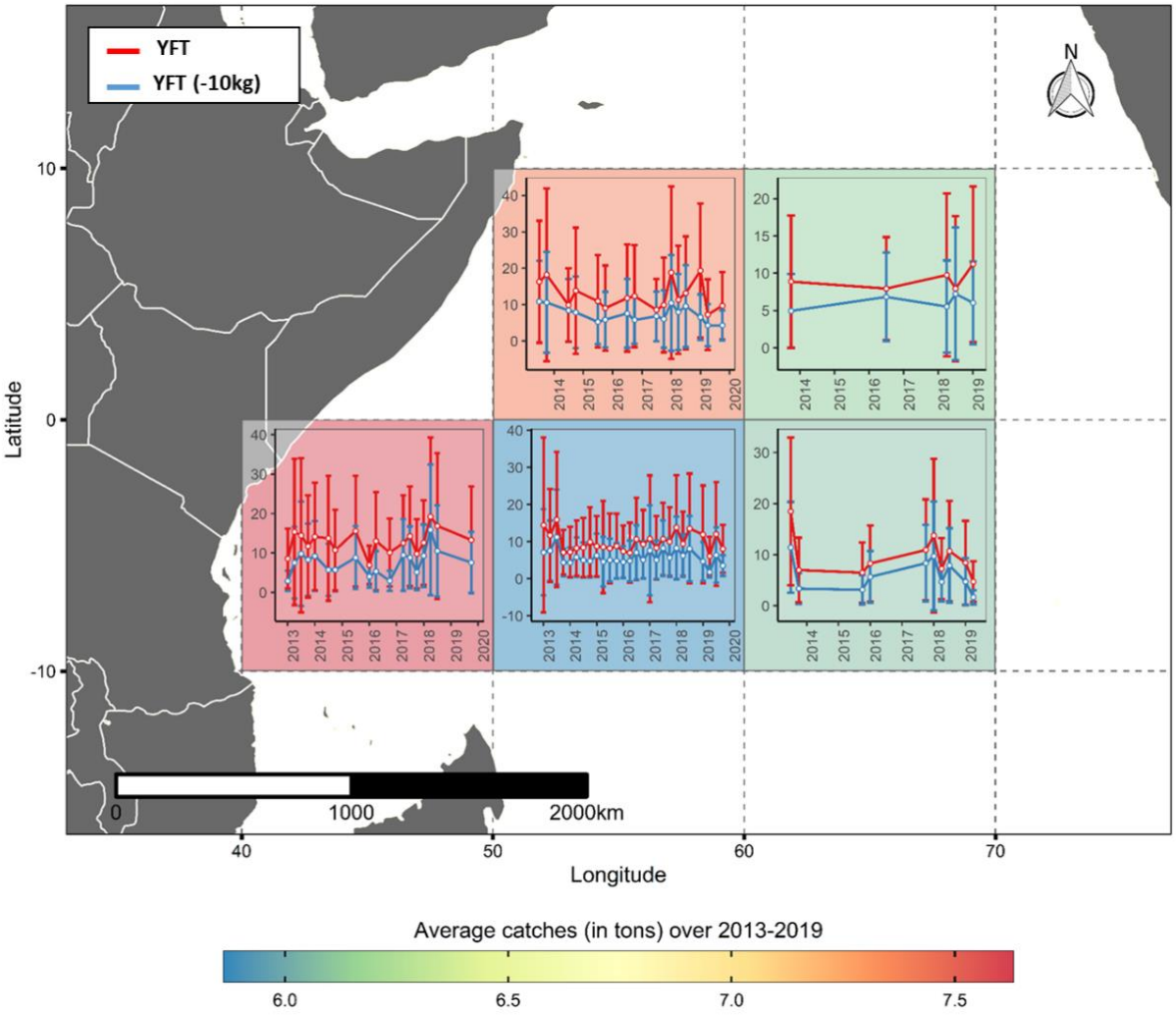

Figure A2.1 : Quarterly averages of total YFT and YFT (-10kg) catches per FOB set across the different time-area units. The background colours indicate to the average YFT (-10kg) catches over 2013-2019.

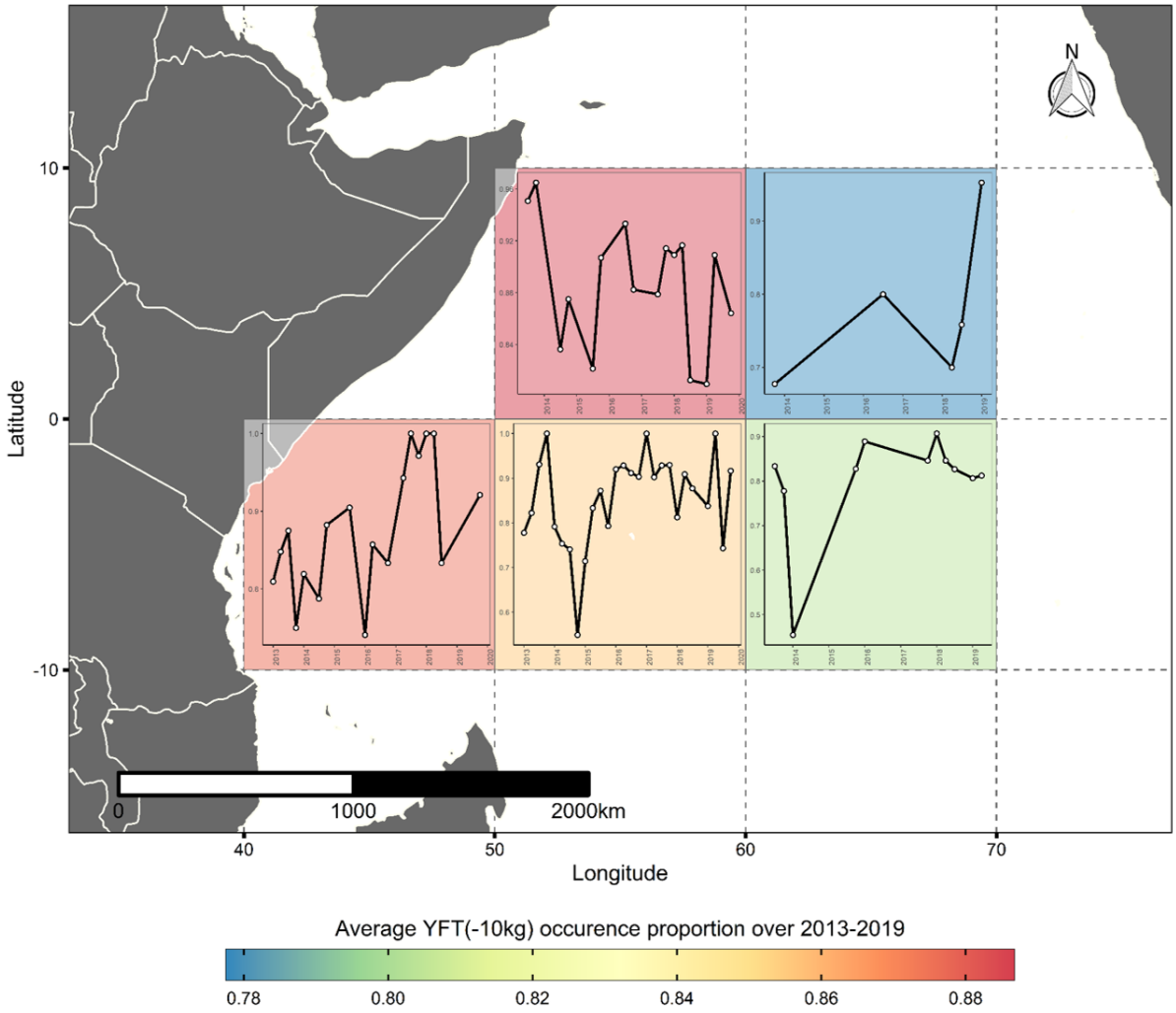

Figure A2.2 : The coefficient η(YFT-10 kg), representing the ratio between the number of DFAD-catches containing a biomass greater than or equal to 1 ton of YFT-10 kg, relative to the total number of sampled DFAD sets, for each spatio-temporal strata. The background colours indicate to the average YFT (-10kg) occurence over 2013-2019.

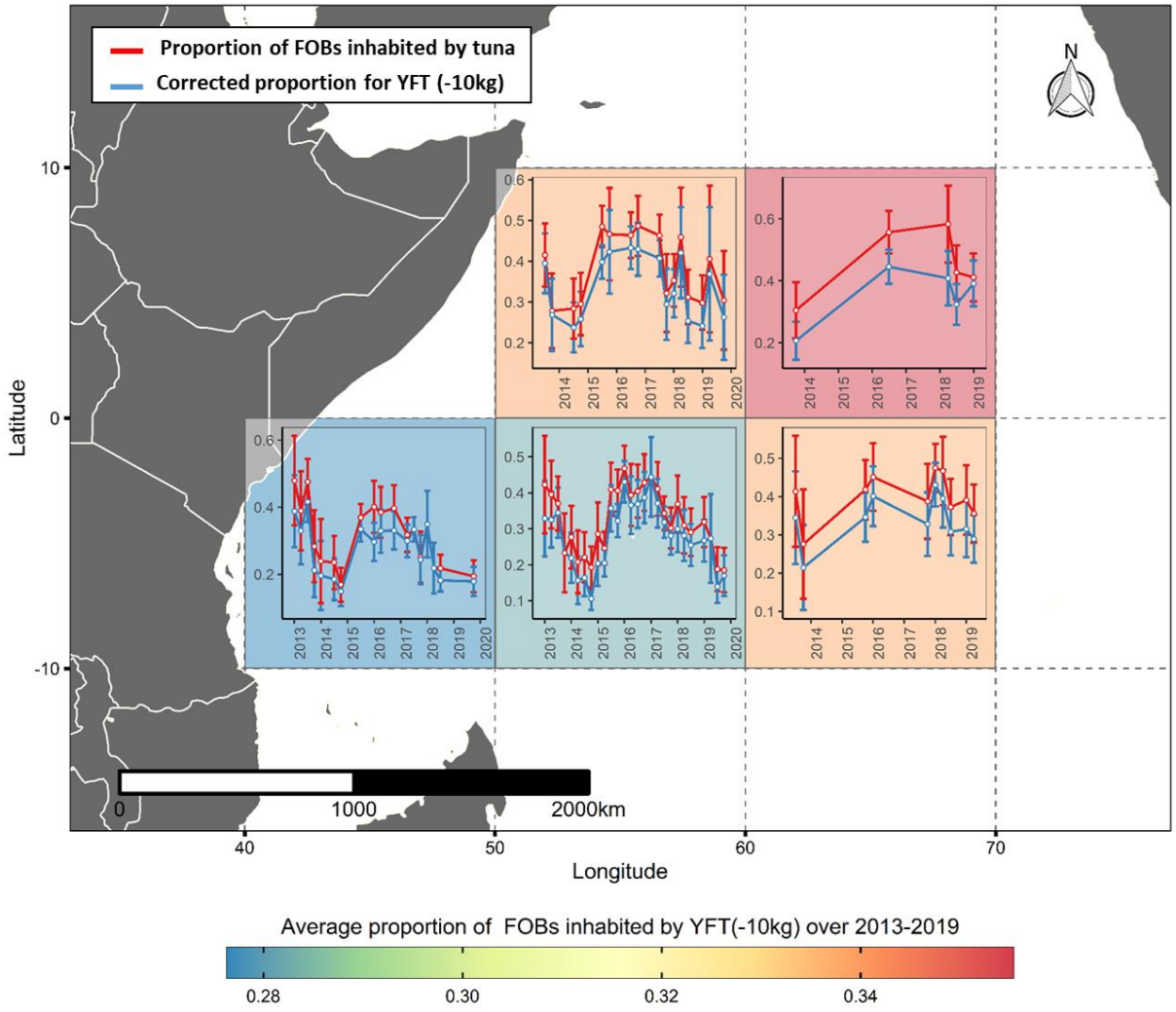

Figure A2.3 : Quarterly averages of proportion of FOBs occupied by tunas (all species) and by YFT-10 kg across the different spatial units. A threshold of 1 ton is considered for assessing whether a FOB is occupied. The background colours indicate to the average proportion of FOBs inhabited by YFT (-10kg) over 2013-2019.

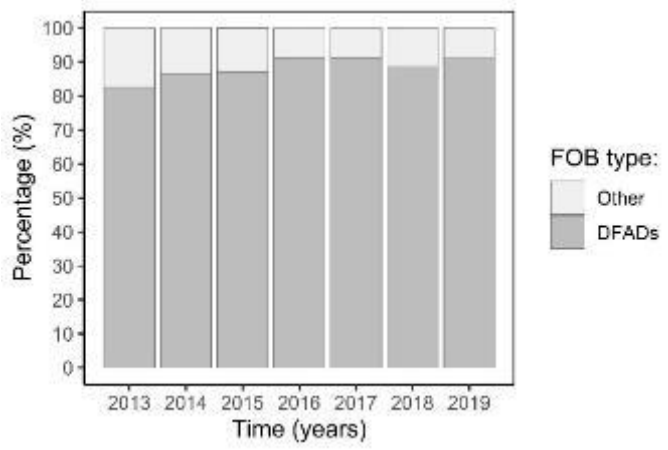

Figure A2.4: Proportions of drifting fish aggregating devices (DFADs) and other types of natural and artificial objects (Other) reported by observers on board French tuna seiners.

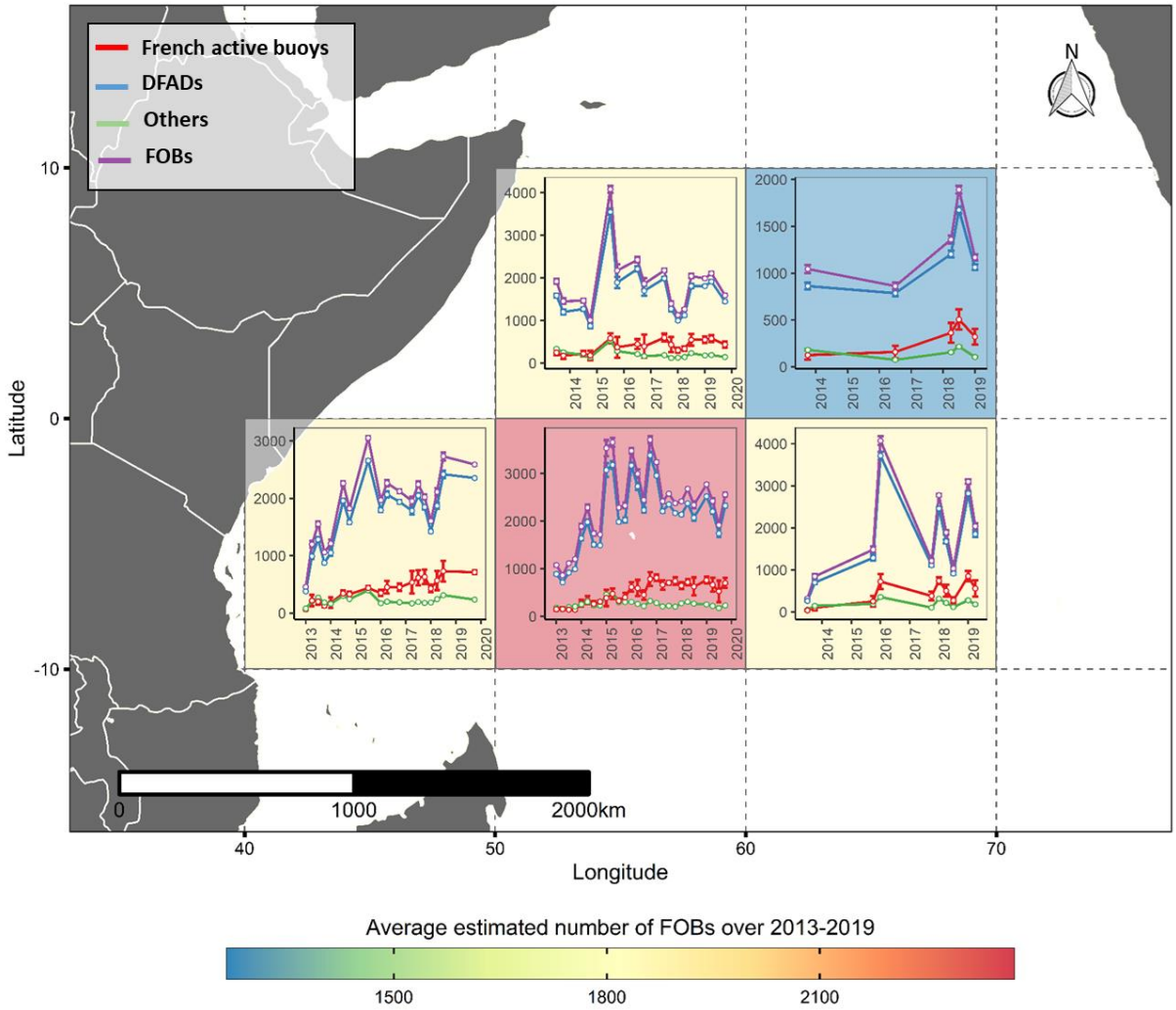

Figure A2.5: Quarterly average of the daily number of the French active buoys, the estimated numbers of drifting fish aggregating devices (DFADs), the others objects (Other), and the estimated total number of floating objects (FOBs) across the different spatial units (FOBs = DFADs + Other). The background colours indicate to the average proportion of FOBs inhabited by YFT (-10kg) over 2013-2019.

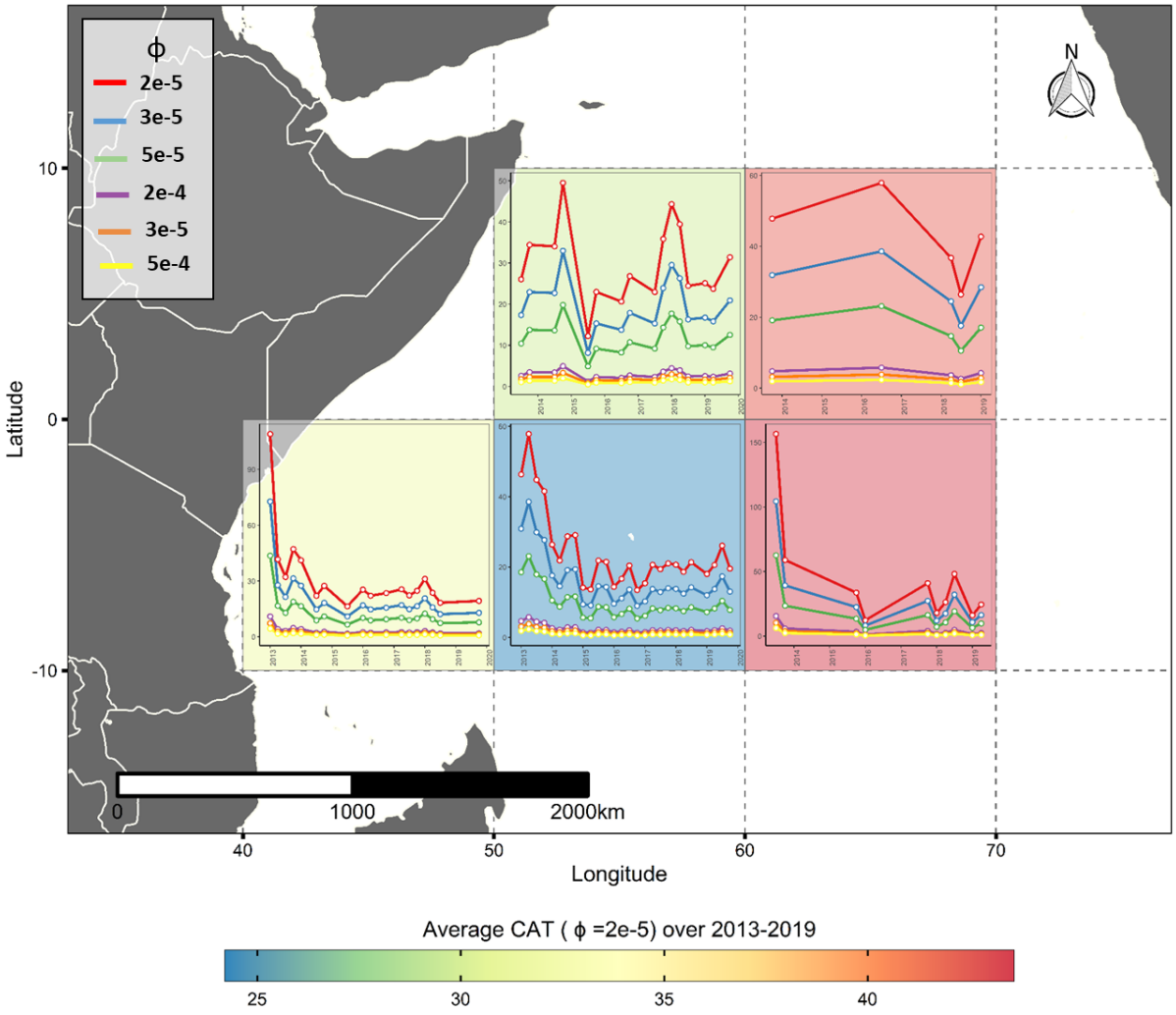

Figure A2.6 : Average CATs estimated for different values of ϕ across the different time-area. The background colours indicate the average CATs (in days) over 2013-2019.

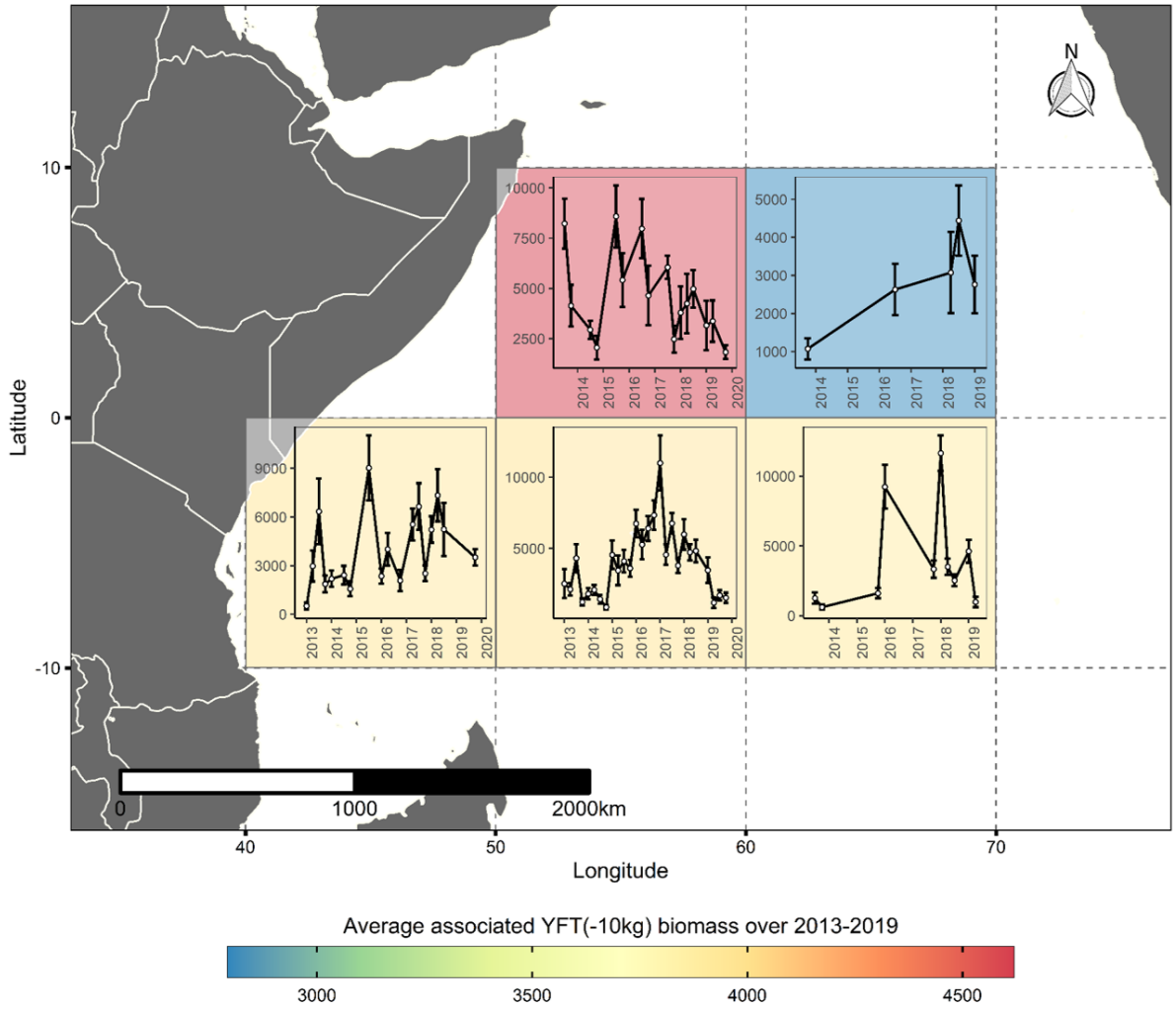

Figure A2.7: Time series of the associated component of YFT-10kg population across the different time-are units (in tons). The background colours indicate the average associated biomass of YFT (-10kg) over 2013-2019.

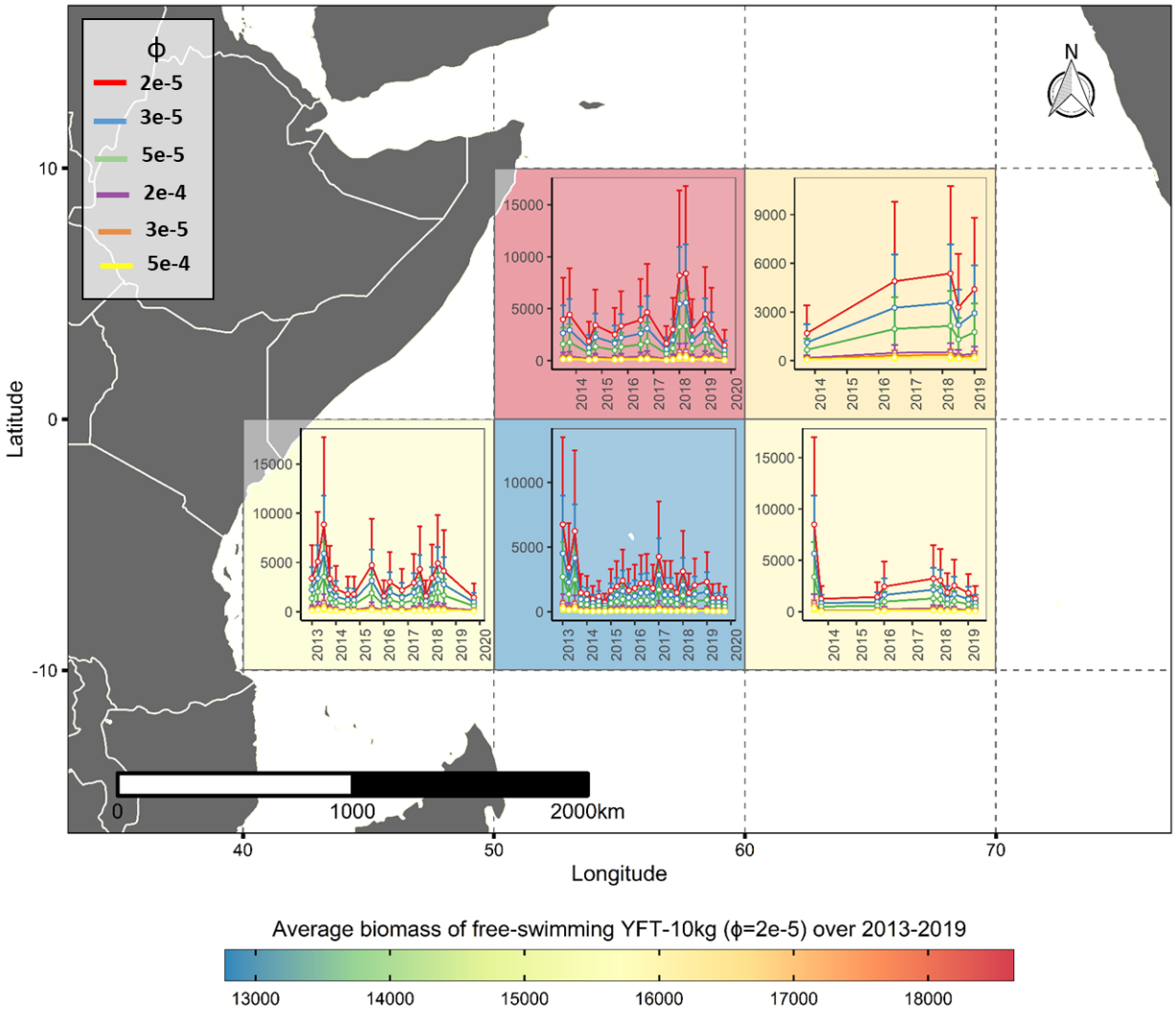

Figure A2.8: Time series of the free-swimming component of YFT-10kg population across the different time-are units under different values of ϕ. The background colours indicate the average free-swimming biomass of YFT (-10kg) over 2013-2019, for ϕ = 2e-5.

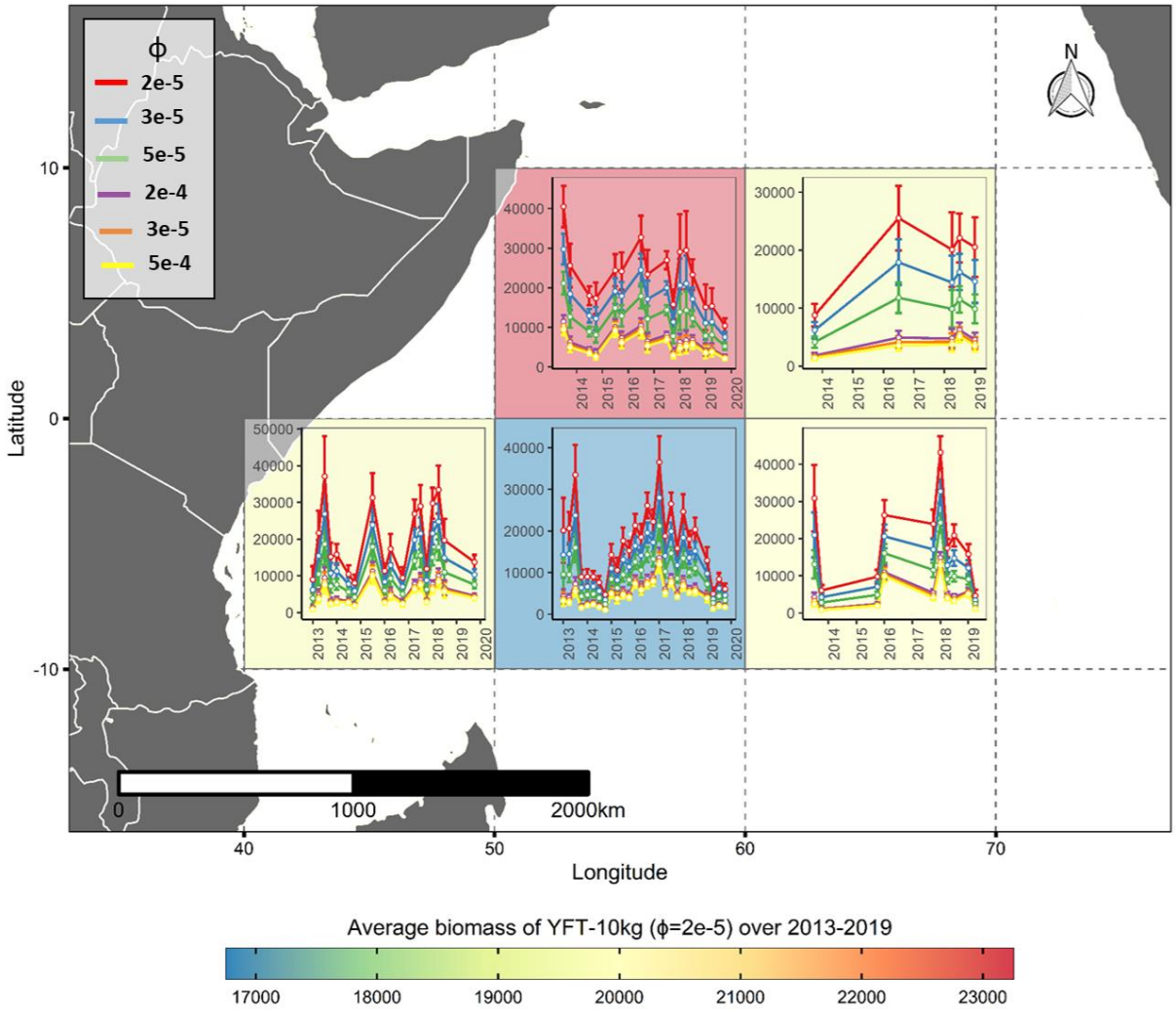

Figure A2.9: Time series of the total population of YFT-10kg across the different time-are units under different values of ϕ. The background colours indicate the average biomass of YFT (-10kg) over 2013-2019, for ϕ = 2e-5.